



Effect of lithium content on electrochemical property of $\text{Li}_{1+x}(\text{Mn}_{0.6}\text{Ni}_{0.2}\text{Co}_{0.2})_{1-x}\text{O}_2$ ($0 \leq x \leq 0.3$) composite cathode materials for rechargeable lithium-ion batteries

Cheng-chi PAN, Ying-chang YANG, Hong-shuai HOU, Ming-jun JING, Yi-rong ZHU, Wei-xin SONG, Xiao-bo JI

College of Chemistry and Chemical Engineering, Central South University, Changsha 410083, China

Received 11 September 2015; accepted 27 April 2016

Abstract: In order to confirm the optimal Li content of Li-rich Mn-based cathode materials (a fixed mole ratio of Mn to Ni to Co is 0.6:0.2:0.2), $\text{Li}_{1+x}(\text{Mn}_{0.6}\text{Ni}_{0.2}\text{Co}_{0.2})_{1-x}\text{O}_2$ ($x=0, 0.1, 0.2, 0.3$) composites were obtained, which had a typical layered structure with $R\bar{3}m$ and $C2/m$ space group observed from X-ray powder diffraction (XRD). Electron microscopy micrograph (SEM) reveals that the particle sizes in the range of 0.4–1.1 μm increase with an increase of x value. $\text{Li}_{1.2}(\text{Mn}_{0.6}\text{Ni}_{0.2}\text{Co}_{0.2})_{0.8}\text{O}_2$ sample delivers a larger initial discharge capacity of 275.7 $\text{mA}\cdot\text{h/g}$ at the current density of 20 mA/g in the potential range of 2.0–4.8 V, while $\text{Li}_{1.1}(\text{Mn}_{0.6}\text{Ni}_{0.2}\text{Co}_{0.2})_{0.9}\text{O}_2$ shows a better cycle performance with a capacity retention of 93.8% at 0.2C after 50 cycles, showing better reaction kinetics of lithium ion insertion and extraction.

Key words: cathode material; $\text{Li}_{1+x}(\text{Mn}_{0.6}\text{Ni}_{0.2}\text{Co}_{0.2})_{1-x}\text{O}_2$; electrochemical property; lithium-ion battery

1 Introduction

Lithium-ion batteries (LIBs) have been extensively used for mobile electronics, plug-in hybrid vehicles (PHEVs) and electric vehicles (EVs) due to their high energy density, excellent conversion efficiency, improved safety and longer cycle life. It is well regarded that the research and promotion of cathode materials are the most effective in the application potential of LIBs. Unfortunately, the layered LiCoO_2 , olivine LiFePO_4 and spinel LiMn_2O_4 have been limited by the relatively low specific capacity in PHEVs and EVs. Even though $\text{Li}[\text{Ni}_{0.8}\text{Co}_{0.1}\text{Mn}_{0.1}]\text{O}_2$ can provide a high capacity of approximately 200 $\text{mA}\cdot\text{h/g}$, it still suffers from inferior cycle life and safety issues. Recently, Li-rich Mn-based compounds have become one of the most promising candidates for cathode materials owing to their high capacity [1,2] (>200 $\text{mA}\cdot\text{h/g}$) when electrochemically activated above 4.4 V by removal of Li_2O from their structure during the initial charge [3–6].

$\text{Li}_{1+x}\text{Mn}_y\text{Ni}_z\text{Co}_{1-x-y-z}\text{O}_2$ has the structural compatibility between the layered Li_2MnO_3 and LiMO_2 ($M=\text{Ni}, \text{Co}, \text{Mn}$) components [7], which allows

integration to occur at the nanoscopic level and the possibility of tailoring the composition of the electrode to achieve optimum performances. Moreover, for $\text{Li}_{1+x}\text{Mn}_y\text{Ni}_z\text{Co}_{1-x-y-z}\text{O}_2$ composites, LiMO_2 component can supply good electrochemical properties such as prolonged cycling life, while Li_2MnO_3 can provide extra Li^+ ions at voltages higher than 4.4 V and simultaneously increase the structural and thermal stabilities [8,9]. However, the electrochemical properties of $\text{Li}_{1+x}\text{Mn}_y\text{Ni}_z\text{Co}_{1-x-y-z}\text{O}_2$ are directly affected by the production routes and the detailed composition of the material. Therefore, various methods like solid-state reaction, co-precipitation method and sol-gel method are introduced to prepare $\text{Li}_{1+x}\text{Mn}_y\text{Ni}_z\text{Co}_{1-x-y-z}\text{O}_2$ composites. JOHNSON et al [10] systematically studied $x\text{Li}_2\text{MnO}_3\cdot(1-x)\text{LiNi}_{1/3}\text{Co}_{1/3}\text{Mn}_{1/3}\text{O}_2$ ($0 \leq x \leq 0.7$) materials prepared by co-precipitation approach. $\text{Li}/0.3\text{Li}_2\text{MnO}_3\cdot 0.7\text{LiNi}_{1/3}\text{Co}_{1/3}\text{Mn}_{1/3}\text{O}_2$ cells with acid-treated electrodes can deliver a high initial discharge capacity of 221 $\text{mA}\cdot\text{h/g}$ in a voltage range of 2.0–4.6 V. TANG et al [2] have also investigated the relationship between lithium content and electrochemical performance of $\text{Li}_{1+x}\text{Ni}_{0.533}\text{Ni}_{0.233}\text{Mn}_{0.233}\text{O}_2$ ($x=0, 0.045, 0.09, 0.135, 0.18, 0.225$). $\text{Li}_{1.09}\text{Ni}_{0.486}\text{Ni}_{0.212}\text{Mn}_{0.212}\text{O}_2$

Foundation item: Project (21473258) supported by the National Natural Science Foundation of China; Project (13JJ1004) supported by Distinguished Young Scientists of Hunan Province, China; Project (NCET-11-0513) supported by Program for the New Century Excellent Talents in University, China

Corresponding author: Xiao-bo JI; Tel: +86-731-88877237; E-mail: xji@csu.edu.cn
DOI: 10.1016/S1003-6326(18)64647-3

sample prepared by a conventional solid-state reaction demonstrates an initial discharge capacity of 231.4 mA·h/g in 40 mA/g between 2.0 and 4.8 V (vs Li/Li⁺) and exhibits the best rate capability. TOPRAKCI [11] et al carefully controlled composition and further examined characterization of various $x\text{Li}_2\text{MnO}_3 \cdot (1-x)\text{LiNi}_{1/3}\text{Co}_{1/3}\text{Mn}_{1/3}\text{O}_2$ ($x=0.1, 0.2, 0.3, 0.4, 0.5$) prepared by the one-step sol-gel route. The as-resulted $0.3\text{Li}_2\text{MnO}_3 \cdot 0.7\text{LiNi}_{1/3}\text{Co}_{1/3}\text{Mn}_{1/3}\text{O}_2$ composite expresses a discharge capacity of 184 mA·h/g and keeps excellent capacity retention of 98% at the 50th cycle. Based on the previous works, there are few studies reported for the optimal Li content with a fixed mole ratio of $n(\text{Mn}):n(\text{Ni}):n(\text{Co})=0.6:0.2:0.2$ in $\text{Li}_{1+x}\text{Mn}_y\text{Ni}_z\text{Co}_{1-x-y-z}\text{O}_2$.

In this work, an improved preparation technique has been adopted to prepare the $\text{Li}_{1+x}(\text{Mn}_{0.6}\text{Ni}_{0.2}\text{Co}_{0.2})_{1-x}\text{O}_2$ ($x=0, 0.1, 0.2, 0.3$) composites by two-step co-precipitation approach. $\text{Li}_{1+x}(\text{Mn}_{0.6}\text{Ni}_{0.2}\text{Co}_{0.2})_{1-x}\text{O}_2$ ($x=0, 0.1, 0.2, 0.3$) composites with fixed $n(\text{Mn}):n(\text{Ni}):n(\text{Co})=0.6:0.2:0.2$ have been systemically studied through optimizing Li content. The effects of lithium content on characteristics of structure, morphology and electrochemical properties were also evaluated. $\text{Li}_{1.1}(\text{Mn}_{0.6}\text{Ni}_{0.2}\text{Co}_{0.2})_{0.9}\text{O}_2$ has the best rate capability with discharge capacity of 145.8 mA·h/g at 2C between 2.0 and 4.8 V.

2 Experimental

Various composite cathode materials $\text{Li}_{1+x}(\text{Mn}_{0.6}\text{Ni}_{0.2}\text{Co}_{0.2})_{1-x}\text{O}_2$ ($x=0, 0.1, 0.2, 0.3$) were prepared by an improved co-precipitation method followed by solid-state reaction. A certain amount of $\text{NiSO}_4 \cdot 6\text{H}_2\text{O}$, $\text{CoSO}_4 \cdot 7\text{H}_2\text{O}$ and $\text{MnSO}_4 \cdot 5\text{H}_2\text{O}$ (1:1:5 molar ratio) were dissolved in the distilled water and slowly dripped into a reactor under a N₂ atmosphere. Concurrently, NaOH solution and NH₃·H₂O solution were added dropwisely by peristaltic pump into the reactor, in which the temperature was held at 50 °C when the concentration, pH, temperature, and stirring speed of the mixture were closely controlled. After completing addition of the transition metal sulfate solution, the reactor temperature was raised to 70 °C, and then an appropriate amount of transition metal sulfate solution ($n(\text{Ni}):n(\text{Co}):n(\text{Mn})=1:1:1$, molar ratio) was put into the continuously stirred reactor under other conditions unchanged. The resultant slurry was aged in a sealed container at 70 °C for 8 h and the precipitates were filtered and washed several times with distilled deionized water, and dried in a vacuum oven at 40 °C for 12 h. Thereafter, the obtained $(\text{Mn}_{0.6}\text{Ni}_{0.2}\text{Co}_{0.2})(\text{OH})_2$ powders and the stoichiometrically required amount of LiOH₂ were thoroughly mixed in ethanol using a mortar and

pestle, the mixture was preheated at 480 °C for 4 h with the heating rate of 4 °C/min in air atmosphere, and then ground and finally sintered at 900 °C for 15 h.

X-ray diffraction (XRD, Cu K_α radiation, Rigaku, Rint-2000) was carried out to identify the crystalline structure in the 2θ range of 10°–80°, with a scan rate of 6 (°)/min. The lattice parameters of $\text{Li}_{1+x}(\text{Mn}_{0.6}\text{Ni}_{0.2}\text{Co}_{0.2})_{1-x}\text{O}_2$ ($x=0, 0.1, 0.2, 0.3$) were calculated from the XRD patterns using the least-squares method. The morphology of the synthesized powders was observed by scanning electron microscopy (SEM, JSM-6510, JEOL, Japan). The precise cation composition of the prepared powders was measured by inductively coupled plasma optical emission spectroscopy (Spectroflame ICP, 2.5 kW, 27 MHz) and is summarized in Table 1.

Table 1 Chemical compositions of expected and prepared powders

Expected	Prepared
$\text{Li}_{1.0}(\text{Mn}_{0.6}\text{Ni}_{0.2}\text{Co}_{0.2})_{1.0}\text{O}_2$	$\text{Li}_{0.96}(\text{Mn}_{0.61}\text{Ni}_{0.19}\text{Co}_{0.22})_{1.07}\text{O}_2$
$\text{Li}_{1.1}(\text{Mn}_{0.6}\text{Ni}_{0.2}\text{Co}_{0.2})_{0.9}\text{O}_2$	$\text{Li}_{1.09}(\text{Mn}_{0.63}\text{Ni}_{0.19}\text{Co}_{0.21})_{0.91}\text{O}_2$
$\text{Li}_{1.2}(\text{Mn}_{0.6}\text{Ni}_{0.2}\text{Co}_{0.2})_{0.8}\text{O}_2$	$\text{Li}_{1.19}(\text{Mn}_{0.64}\text{Ni}_{0.19}\text{Co}_{0.22})_{0.79}\text{O}_2$
$\text{Li}_{1.3}(\text{Mn}_{0.6}\text{Ni}_{0.2}\text{Co}_{0.2})_{0.7}\text{O}_2$	$\text{Li}_{1.28}(\text{Mn}_{0.65}\text{Ni}_{0.18}\text{Co}_{0.23})_{0.68}\text{O}_2$

The positive electrodes for the electrochemical studies were prepared by mixing active materials, carbon black and polyvinylidene fluoride (80:10:10, mass ratio) in N-methyl-pyrrolidone. The obtained slurry was coated onto aluminum foil and dried in a vacuum oven at 110 °C for 12 h. Coin cells (CR2016, diameter=20 mm) were assembled in an argon filled glove box (MB-Labstar 1200/780, M.Braun Inertgas-Systeme GmbH, Germany) with 1 mol/L LiPF₆ dissolved in EC/DMC/EMC (1:1:1, volume ratio, PANAX ETEC Co. Ltd, Korea). Coin cells were galvanostatically charged/discharged on BT2000 battery testing system (BT2000-10V10A8CH, ARBIN Corporation, USA) in the voltage range of 2.0–4.8 V (vs Li) (0.1C=20 mA/g) at room temperature. Electrochemical impedance spectra (EIS) measurements were carried out in the frequency range of 0.1 Hz–100 kHz using a vibration voltage of 5 mV to determine the resistance of the cycled cells.

3 Results and discussion

The nominal compositions of $\text{Li}_{1+x}(\text{Mn}_{0.6}\text{Ni}_{0.2}\text{Co}_{0.2})_{1-x}\text{O}_2$ ($x=0, 0.1, 0.2, 0.3$) samples are presented in Table 1, indicating that the average chemical compositions of the as-obtained materials are very similar to the targeted stoichiometry. Powder XRD patterns of cathode material $\text{Li}_{1+x}(\text{Mn}_{0.6}\text{Ni}_{0.2}\text{Co}_{0.2})_{1-x}\text{O}_2$ ($x=0, 0.1, 0.2, 0.3$) are shown in Fig. 1. Compared with

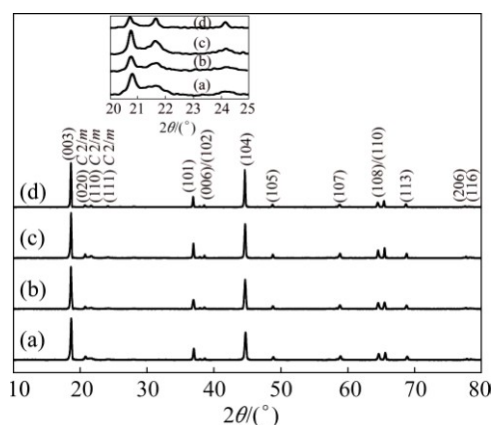


Fig. 1 XRD patterns of as-prepared $\text{Li}_{1+x}(\text{Mn}_{0.6}\text{Ni}_{0.2}\text{Co}_{0.2})_{1-x}\text{O}_2$: (a) $x=0$; (b) $x=0.1$; (c) $x=0.2$; (d) $x=0.3$

layered materials $\text{LiNi}_x\text{Co}_y\text{Mn}_{1-x-y}\text{O}_2$, it is well-known that the key distinction in XRD patterns is that Li-rich layered materials $\text{Li}_{1+x}\text{Mn}_y\text{Ni}_z\text{Co}_{1-x-y-z}\text{O}_2$ have weak diffraction peaks. All the strong diffraction peaks show the hexagonal $\alpha\text{-NaFeO}_2$ structure (space group: $R3m$). The splitting of the diffraction peaks (006)/(102) and (108)/(110) in the XRD patterns are clearly separated, suggesting that the layer structures have good hexagonal ordering. Meanwhile, the magnified XRD patterns between 20° and 25° represent the existence of Li_2MnO_3 phase ($C2/m$). Furthermore, the peaks at 20° to 25° became better defined while x increases from 0 to 0.3, which expresses that the Li_2MnO_3 phase in the composites gets increased content and/or improved crystallinity [12,13].

Table 2 illustrates the structural parameters and c/a ratios of as-prepared $\text{Li}_{1+x}(\text{Mn}_{0.6}\text{Ni}_{0.2}\text{Co}_{0.2})_{1-x}\text{O}_2$ ($x=0, 0.1, 0.2, 0.3$) calculated by XRD data. The c/a ratio is attributed largely to difference in the relative ratios of change in lattice parameters a and c . It was found that the values of a , c , c/a and unit cell volume V increased with the increased Li content in $\text{Li}_{1+x}(\text{Mn}_{0.6}\text{Ni}_{0.2}\text{Co}_{0.2})_{1-x}\text{O}_2$, which can be attributed to the increased content of Li_2MnO_3 (Li^+ , 0.68 \AA), leading to the increasing Mn^{4+} (0.53 \AA) concentration from partial reduction of Mn^{3+} (0.65 \AA) caused by balancing the cation and anion in $\text{Li}_{1+x}(\text{Mn}_{0.6}\text{Ni}_{0.2}\text{Co}_{0.2})_{1-x}\text{O}_2$.

Figure 2 describes the morphologies of $\text{Li}_{1+x}(\text{Mn}_{0.6}\text{Ni}_{0.2}\text{Co}_{0.2})_{1-x}\text{O}_2$ ($x=0, 0.1, 0.2, 0.3$) composites. SEM

images clearly reveal that the powders consist of particles with no obvious aggregation, which have the size distribution between 0.4 and 1.2 μm . Moreover, the $\text{Li}_{1.1}(\text{Mn}_{0.6}\text{Ni}_{0.2}\text{Co}_{0.2})_{0.9}\text{O}_2$ exhibits narrower size distribution with the average particle size of 0.7 μm . As can be seen from Fig. 2, the particles undergo gradual increase in particle size with increase of x value, and the main reason is that excess LiOH accelerates grain growth, which could lengthen the lithium ion diffusion path and further influence the electrochemical performance of cathode material.

Figure 3 illustrates the initial voltage versus capacity curves on charge and discharge at a current density of 20 mA/g (0.1C rate) within the potential range of 2.0–4.8 V. It suggests that the initial charge process below 4.5 V is ascribed to the removal of lithium from the electrode structure accompanied with the oxidation of the Ni^{2+} and Co^{3+} , where the four composites exhibit similar curve. While, the initial charge process above 4.5 V can be attributed to the activation of inactive Li_2MnO_3 content associated with the irreversible extraction of Li_2O from the composites. The initial charge capacities are 323.1, 359, 364.9 and 380.9 mA·h/g, respectively, for $\text{Li}_{1+x}(\text{Mn}_{0.6}\text{Ni}_{0.2}\text{Co}_{0.2})_{1-x}\text{O}_2$ ($x=0, 0.1, 0.2, 0.3$) composites, and the initial discharge capacities are 230.5, 267.4, 275.7 and 245.4 mA·h/g, respectively, for $\text{Li}_{1+x}(\text{Mn}_{0.6}\text{Ni}_{0.2}\text{Co}_{0.2})_{1-x}\text{O}_2$ ($x=0, 0.1, 0.2, 0.3$) composites. Among all four composites, $\text{Li}_{1.2}(\text{Mn}_{0.6}\text{Ni}_{0.2}\text{Co}_{0.2})_{0.8}\text{O}_2$ reaches a relatively high coulombic efficiency of 75.6%.

Figure 4 indicates the cycling performance of the $\text{Li}/\text{Li}_{1+x}(\text{Mn}_{0.6}\text{Ni}_{0.2}\text{Co}_{0.2})_{1-x}\text{O}_2$ ($x=0, 0.1, 0.2, 0.3$) cells between 2.0 and 4.8 V at a constant current density of 40 mA/g (0.2C rate). Each cell was firstly charged/discharge galvanostatically at 0.1C for three cycles. It is clear that the Li_2MnO_3 content is considerable in determining the electrochemical performance of the composites. It can be found that as the value x increases from 0 to 0.3, the capacity retentions of the $\text{Li}_{1+x}(\text{Mn}_{0.6}\text{Ni}_{0.2}\text{Co}_{0.2})_{1-x}\text{O}_2$ composites are 91.8%, 93.8%, 92.9% and 87.3%, after 50 cycles, and the initial discharge capacities are 200.5, 227.4, 235.7 and 215.4 mA·h/g, respectively. $\text{Li}_{1+x}(\text{Mn}_{0.6}\text{Ni}_{0.2}\text{Co}_{0.2})_{1-x}\text{O}_2$ composites showed that the capacity increased gradually with the increase of Li content in the x range of 0–0.2, and then decreased with an increase of Li content in the x

Table 2 Structural parameters and c/a ratios of $\text{Li}_{1+x}(\text{Mn}_{0.6}\text{Ni}_{0.2}\text{Co}_{0.2})_{1-x}\text{O}_2$

x	$a/\text{\AA}$	$c/\text{\AA}$	c/a	$V/\text{\AA}^3$
0	2.8510(3)	14.1985(5)	0.200797	100.23
0.1	2.8604(9)	14.2046(6)	0.201377	100.66
0.02	2.8706(2)	14.2176(0)	0.201906	101.88
0.2	2.8794(2)	14.2228(8)	0.20245	102.12

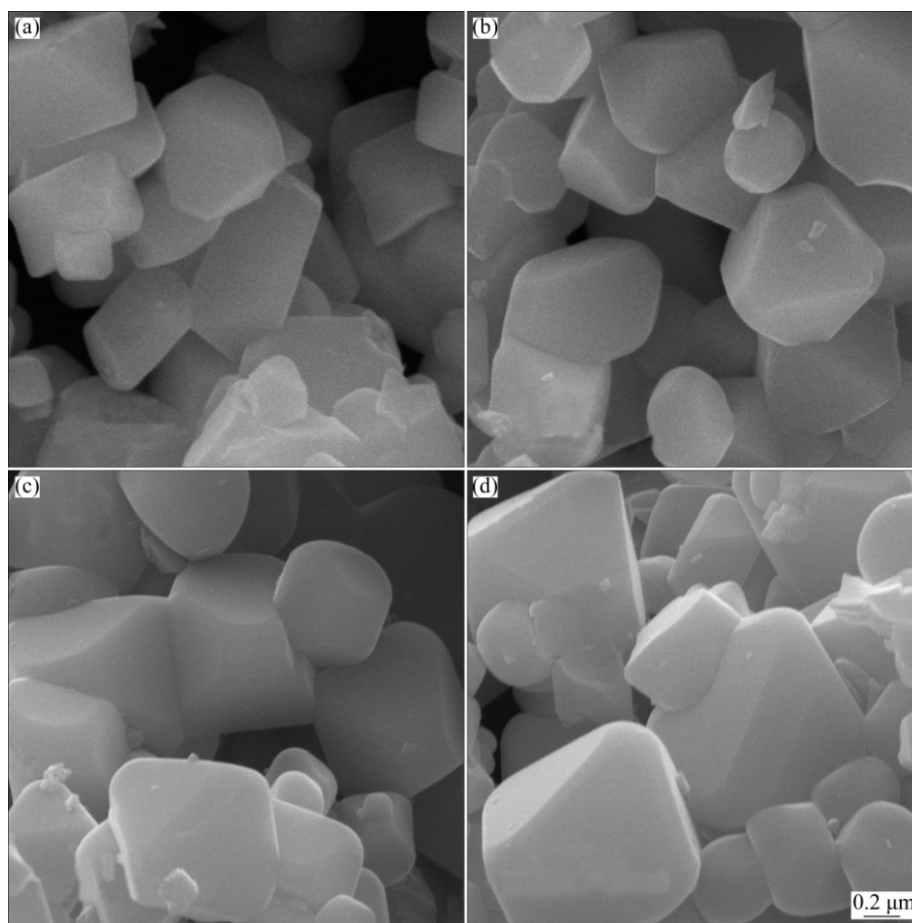


Fig. 2 SEM images of $\text{Li}_{1+x}(\text{Mn}_{0.6}\text{Ni}_{0.2}\text{Co}_{0.2})_{1-x}\text{O}_2$: (a) $x=0$; (b) $x=0.1$; (c) $x=0.2$; (d) $x=0.3$

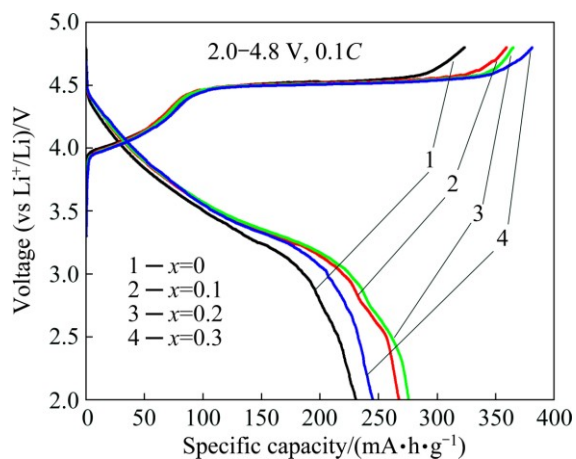


Fig. 3 Initial charge–discharge capacities of $\text{Li}/\text{Li}_{1+x}(\text{Mn}_{0.6}\text{Ni}_{0.2}\text{Co}_{0.2})_{1-x}\text{O}_2$ cells with current density of 40 mA/g between 2.0 and 4.8 V at 25 °C

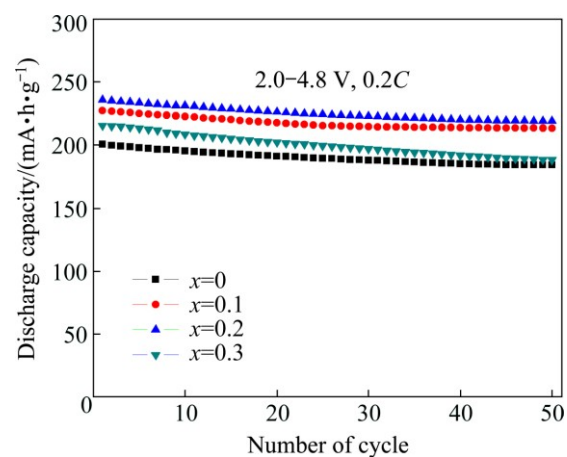


Fig. 4 Discharge capacity vs number of cycles of $\text{Li}/\text{Li}_{1+x}(\text{Mn}_{0.6}\text{Ni}_{0.2}\text{Co}_{0.2})_{1-x}\text{O}_2$ cells in voltage range of 2.0–4.8 V at 25 °C

range of 0.2–0.3, which can be primarily ascribed to an appropriate amount of Li_2MnO_3 introduced into the structure. This makes their structure stable and improves the cycling performance, while superfluous Li_2MnO_3 results from irregular crystal grain growth, large polarization and gradual transformation from the layered structure to a spinel-like phase in $\text{Li}_{1.3}(\text{Mn}_{0.6}\text{Ni}_{0.2}\text{Co}_{0.2})_{0.7}\text{O}_2$

O_2 sample. Although $\text{Li}_{1.2}(\text{Mn}_{0.6}\text{Ni}_{0.2}\text{Co}_{0.2})_{0.8}\text{O}_2$ delivers the highest discharge capacity of 235.7 mA·h/g, $\text{Li}_{1.1}(\text{Mn}_{0.6}\text{Ni}_{0.2}\text{Co}_{0.2})_{0.9}\text{O}_2$ shows a better capacity retention of 93.8%.

The rate capability test of the $\text{Li}/\text{Li}_{1+x}(\text{Mn}_{0.6}\text{Ni}_{0.2}\text{Co}_{0.2})_{1-x}\text{O}_2$ ($x=0, 0.1, 0.2, 0.3$) cells is presented in Fig. 5. Each cell was firstly charged/discharged galvano-

statically at 0.1C (20 mA/g) for three cycles, at 0.2C, 0.5C, 1C, 2C, 0.2C for every cycle, respectively. As can be seen in Fig. 5, the rate capability of $\text{Li}_{1+x}(\text{Mn}_{0.6}\text{Ni}_{0.2}\text{Co}_{0.2})_{1-x}\text{O}_2$ ($x=0, 0.1, 0.2, 0.3$) firstly gets better and then deteriorates with the increase of x value. $\text{Li}_{1.1}(\text{Mn}_{0.6}\text{Ni}_{0.2}\text{Co}_{0.2})_{0.9}\text{O}_2$ and $\text{Li}_{1.2}(\text{Mn}_{0.6}\text{Ni}_{0.2}\text{Co}_{0.2})_{0.8}\text{O}_2$ cells demonstrate slightly better rate capability. For example, $\text{Li}_{1.2}(\text{Mn}_{0.6}\text{Ni}_{0.2}\text{Co}_{0.2})_{0.8}\text{O}_2$ samples have 235.4, 201.4, 180.7, 142.1 mA·h/g, respectively, at 0.2C, 0.5C, 1C, 2C. Meanwhile, $\text{Li}(\text{Mn}_{0.6}\text{Ni}_{0.2}\text{Co}_{0.2})\text{O}_2$ and $\text{Li}_{1.3}(\text{Mn}_{0.6}\text{Ni}_{0.2}\text{Co}_{0.2})_{0.7}\text{O}_2$ exhibit inferior performance at high rates. In addition, their discharge capacity is lower than 100 mA·h/g at 2C, which is closely related to the unstable structure and high polarization of the material at high currents.

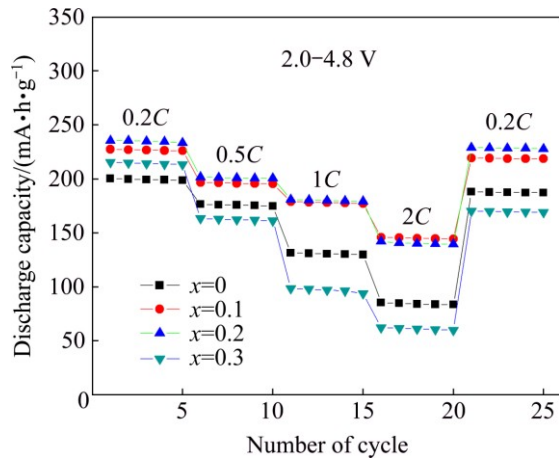


Fig. 5 Comparison of rate capability of $\text{Li}/\text{Li}_{1+x}(\text{Mn}_{0.6}\text{Ni}_{0.2}\text{Co}_{0.2})_{1-x}\text{O}_2$ cells at different rates between 2.0 and 4.8 V at 25 °C

Electrochemical impedance spectroscopy (EIS) measurement has been conducted over the frequency range from 0.1 Hz to 100 kHz with an AC voltage signal of ± 5 mV for $\text{Li}/\text{Li}_{1+x}(\text{Mn}_{0.6}\text{Ni}_{0.2}\text{Co}_{0.2})_{1-x}\text{O}_2$ ($x=0, 0.1, 0.2, 0.3$) cells. The $\text{Li}/\text{Li}_{1+x}(\text{Mn}_{0.6}\text{Ni}_{0.2}\text{Co}_{0.2})_{1-x}\text{O}_2$ ($x=0, 0.1, 0.2, 0.3$) cells underwent 50 cycles at 0.2C between 2.0 and 4.8 V and then fully charged to 4.8 V. As can be seen from Fig. 6, all the impedance spectra have two parts, which are a depressed semicircle in high frequency region related to the charge transfer process (R_{CT}) and a sloping line in low frequency region corresponding to the diffusion behavior of lithium ions in the bulk of the material or also called Warburg resistance (W) [14–16]. In addition, the intercept in high frequency to the real axis is ascribed to the ohmic resistance of electrolyte (R_S), and constant phase-angle element is associated to the non-ideal double layer capacitance (C_{DL}). The impedance parameters calculated from the EIS curves are given in Table 3. It is clear that $\text{Li}_{1+x}(\text{Mn}_{0.6}\text{Ni}_{0.2}\text{Co}_{0.2})_{1-x}\text{O}_2$ ($x=0, 0.1, 0.2, 0.3$) composites have a similar R_S and the values of R_{CT} are 313.9, 196.6, 244.8, 376.4 Ω ,

respectively. It should be noted that $\text{Li}_{1.1}(\text{Mn}_{0.6}\text{Ni}_{0.2}\text{Co}_{0.2})_{0.9}\text{O}_2$ has the lowest R_{CT} value, which plays a dominant role on the impedance parameter and rate capability [17]. The bulk structural irreversible phase transition changes result in the increase of impedance [18], which indicates that $\text{Li}_{1.1}(\text{Mn}_{0.6}\text{Ni}_{0.2}\text{Co}_{0.2})_{0.9}\text{O}_2$ composite possesses better reaction kinetics of lithium ion insertion and extraction than others.

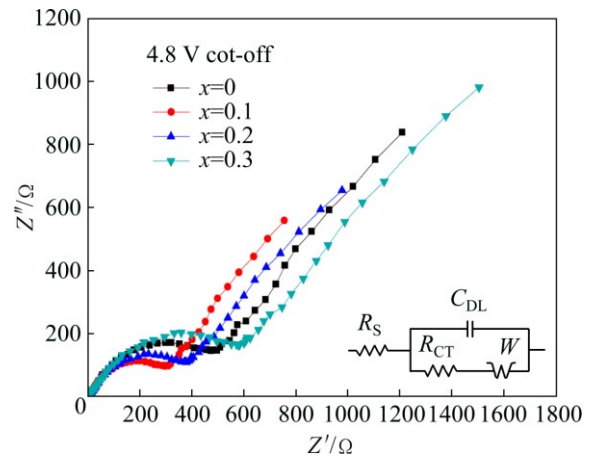


Fig. 6 Nyquist plots of $\text{Li}/\text{Li}_{1+x}(\text{Mn}_{0.6}\text{Ni}_{0.2}\text{Co}_{0.2})_{1-x}\text{O}_2$ cells after 50 cycles at 0.2C under 4.8 V

Table 3 Impedance parameters of $\text{Li}/\text{Li}_{1+x}(\text{Mn}_{0.6}\text{Ni}_{0.2}\text{Co}_{0.2})_{1-x}\text{O}_2$ cells after 50 cycles

x	R_S/Ω	R_{CT}/Ω	$C_{DL}/10^{-6}\text{F}$	$W/(\text{S}\cdot\text{S}^{0.5})$
0	7.584	313.9	1.72	0.1005×10^{-2}
0.1	7.148	196.6	2.587	0.1557×10^{-2}
0.2	7.253	244.8	2.194	0.125×10^{-2}
0.3	7.641	376.4	1.459	0.8216×10^{-3}

4 Conclusions

1) $\text{Li}_{1+x}(\text{Mn}_{0.6}\text{Ni}_{0.2}\text{Co}_{0.2})_{1-x}\text{O}_2$ ($x=0, 0.1, 0.2, 0.3$) composite cathode materials have been successfully prepared utilizing an improved co-precipitation method. The structure and morphology indicate that $\text{Li}_{1+x}(\text{Mn}_{0.6}\text{Ni}_{0.2}\text{Co}_{0.2})_{1-x}\text{O}_2$ ($0\leq x\leq 0.3$) composites show pure phase and compatible structure merged by layered Li_2MnO_3 and LiMO_2 ($M=\text{Ni}, \text{Co}, \text{Mn}$) components. The XRD results between 20° and 25° reveal that the higher the lithium content in the composites is, the better defined the Li_2MnO_3 phase becomes, which indicates that the Li_2MnO_3 phase improves crystallinity. SEM images clearly reveal that the morphologies of the samples tend to grow up and distribute unevenly with increasing lithium content.

2) Although $\text{Li}_{1.2}(\text{Mn}_{0.6}\text{Ni}_{0.2}\text{Co}_{0.2})_{0.8}\text{O}_2$ shows the largest discharge capacity of 235.7 mA·h/g at 40 mA/g and reaches a relatively high coulombic efficiency of 75.6%, $\text{Li}_{1.1}(\text{Mn}_{0.6}\text{Ni}_{0.2}\text{Co}_{0.2})_{0.9}\text{O}_2$ gives the best capacity

retention of 93.8% at 40 mA/g after 50 cycles and has better reaction kinetics of lithium ion insertion and extraction.

References

- [1] GUO Xiao-jian, LI Yi-xiao, ZHENG Min, ZHENG Jian-ming, LI Jie, GONG Zheng-liang, YANG Yong. Structural and electrochemical characterization of $x\text{Li}[\text{Li}_{1/3}\text{Mn}_{2/3}]\text{O}_2 \cdot (1-x)\text{Li}[\text{Ni}_{1/3}\text{Mn}_{1/3}\text{Co}_{1/3}]\text{O}_2$ ($0 \leq x \leq 0.9$) as cathode materials for lithium ion batteries [J]. Journal of Power Sources, 2008, 184(2): 414–419.
- [2] TANG Zhao-hui, WANG Zhi-xing, LI Xin-hai, PENG Wen-jie. Influence of lithium content on the electrochemical performance of $\text{Li}_{1+x}(\text{Mn}_{0.533}\text{Ni}_{0.233}\text{Co}_{0.233})_{1-x}\text{O}_2$ cathode materials [J]. Journal of Power Sources, 2012, 208 (15): 237–241.
- [3] JOHNSON C S, LI Nai-chao, LEFIEF C, THACKERAY M M. Anomalous capacity and cycling stability of $x\text{Li}_2\text{MnO}_3 \cdot (1-x)\text{LiMO}_2$ electrodes (M=Mn, Ni, Co) in lithium batteries at 50 °C [J]. Electrochemistry Communications, 2007, 9(4): 787–795.
- [4] ARUNKUMAR T A, WU Y, MANTHIRAM A. Factors influencing the irreversible oxygen loss and reversible capacity in layered $\text{Li}[\text{Li}_{1/3}\text{Mn}_{2/3}]\text{O}_2$ - $\text{Li}[\text{M}]\text{O}_2$ (M= $\text{Mn}_{0.5-y}\text{Ni}_{0.5-y}\text{Co}_y$ and $\text{Ni}_{1-y}\text{Co}_y$) solid solutions [J]. Chemistry of Materials, 2007, 19 (12): 3067–3073.
- [5] THACKERAY M M, KANG S H, JOHNSON C S, VAUGHNEY J T, BENEDEK R, HACKNEY S A. Li_2MnO_3 -stabilized LiMO_2 (M= Mn, Ni, Co) electrodes for lithium-ion batteries [J]. Journal of Materials Chemistry, 2007, 17 (30): 3112–3125.
- [6] ARMSTRONG A R, HOLZAPFEL M, NOVAK P, JOHNSON C S, KANG S H, THACKERAY M M, BRUCE P G. Demonstrating oxygen loss and associated structural reorganization in the lithium battery cathode $\text{Li}[\text{Ni}_{0.2}\text{Li}_{0.2}\text{Mn}_{0.6}]\text{O}_2$ [J]. Journal of the American Chemical Society, 2006, 128 (26): 8694–8698.
- [7] YABUUCHI N, YOSHII K, MYUNG S T, NAKAI I, KOMABA S. Detailed studies of a high-capacity electrode material for rechargeable batteries, $\text{Li}_2\text{MnO}_3 \cdot \text{LiCo}_{1/3}\text{Ni}_{1/3}\text{Mn}_{1/3}\text{O}_2$ [J]. Journal of the American Chemical Society, 2011, 133(12): 4404–4419.
- [8] CHOI N S, CHEN Zong-hai, FREUNBERGER S A, JI Xiu-lei, SUN Y K, AMINE K, YUSHIN G, NAZAR L F, CHO J, BRUCE P G. Challenges facing lithium batteries and electrical double-layer capacitors [J]. Angewandte Chemie International Edition, 2012, 51(40): 9994–10024.
- [9] DENG Hai-xia, BELHAROUAK I, SUN Y, AMINE K. $\text{Li}_x\text{Ni}_{0.25}\text{Mn}_{0.75}\text{O}_y$ ($0.5 \leq x \leq 2$, $2 \leq y \leq 2.75$) compounds for high-energy lithium-ion batteries [J]. Journal of Materials Chemistry, 2009, 19(26): 4510–4516.
- [10] JOHNSON C S, LI Nai-chao, LEFIEF C, VAUGHNEY J T, THACKERAY M M. Synthesis, characterization and electrochemistry of lithium battery electrodes: $x\text{Li}_2\text{MnO}_3 \cdot (1-x)\text{LiMn}_{0.333}\text{Ni}_{0.333}\text{Co}_{0.333}\text{O}_2$ ($0 \leq x \leq 0.7$) [J]. Chemistry of Materials, 2008, 20(19): 6095–6106.
- [11] TOPRAKCI O, TOPRAKCI H A, LI Ying, JI Li-wen, XUE Lei-gang, LEE H, ZHANG Shu, ZHANG Xiang-wu. Synthesis and characterization of $x\text{Li}_2\text{MnO}_3 \cdot (1-x)\text{LiMn}_{1/3}\text{Ni}_{1/3}\text{Co}_{1/3}\text{O}_2$ composite cathode materials for rechargeable lithium-ion batteries [J]. Journal of Power Sources, 2013, 241(1): 522–528.
- [12] KIM S, KIM C, NOH J K, YU S, KIM S J, CHANG W, CHOI W C, CHUNG K Y, CHO B W. Synthesis of layered-layered $x\text{Li}_2\text{MnO}_3 \cdot (1-x)\text{LiMO}_2$ (M=Mn, Ni, Co) nanocomposite electrodes materials by mechanochemical process [J]. Journal of Power Sources, 2012, 220(15): 422–429.
- [13] KIM J H, PARK C W, SUN Y K. Synthesis and electrochemical behavior of $\text{Li}[\text{Li}_{0.1}\text{Ni}_{0.35-x/2}\text{Co}_x\text{Mn}_{0.55-x/2}]\text{O}_2$ cathode materials [J]. Solid State Ionics, 2003, 164(1): 43–49.
- [14] GAO Fei, TANG Zhi-yuan. Kinetic behavior of LiFePO_4/C cathode material for lithium-ion batteries [J]. Electrochimica Acta, 2008, 53(15): 5071–5075.
- [15] LIU H, LI C, ZHANG H P, FU L J, WU Y P, WU H Q. Kinetic study on LiFePO_4/C nanocomposites synthesized by solid state technique [J]. Journal of Power Sources, 2006, 159(1): 717–720.
- [16] TOPRAKCI O, TOPRAKCI H A, JI Li-wen, XU Guan-jie, LIN Zhan, ZHANG Xiang-wu. Carbon nanotube-loaded electrospun $\text{LiFePO}_4/\text{carbon}$ composite nanofibers as stable and binder-free cathodes for rechargeable lithium-ion batteries [J]. ACS Applied Materials & Interfaces, 2012, 4(3): 1273–1280.
- [17] GAO Min, LIAN Fang, LIU Hong-quan, TIAN Cui-jun, MA Lei-lei, YANG Wang-yue. Synthesis and electrochemical performance of long lifespan Li-rich $\text{Li}_{1+x}(\text{Ni}_{0.37}\text{Mn}_{0.63})_{1-x}\text{O}_2$ cathode materials for lithium-ion batteries [J]. Electrochimica Acta, 2013, 95: 87–94.
- [18] JIN Xue, XU Quan-jie, YUAN Xiao-lei, ZHOU Luo-zeng, XIA Yong-yao. Synthesis, characterization and electrochemical performance of $\text{Li}[\text{Li}_{0.2}\text{Mn}_{0.54}\text{Ni}_{0.13}\text{Co}_{0.13}]\text{O}_2$ cathode materials for lithium-ion batteries [J]. Electrochimica Acta, 2013, 114(30): 605–610.

锂离子电池复合正极材料

$\text{Li}_{1+x}(\text{Mn}_{0.6}\text{Ni}_{0.2}\text{Co}_{0.2})_{1-x}\text{O}_2$ ($0 \leq x \leq 0.3$) 中 锂含量对电化学性能的影响

潘成迟, 杨应昌, 侯红帅, 景明俊, 朱裔荣, 宋维鑫, 纪致波

中南大学 化学化工学院, 长沙 410083

摘要: 为了确定具有固定比例的富锂锰基($\text{Mn}:\text{Ni}:\text{Co}=0.6:0.2:0.2$)正极材料中的最优锂含量, 制备了 $\text{Li}_{1+x}(\text{Mn}_{0.6}\text{Ni}_{0.2}\text{Co}_{0.2})_{1-x}\text{O}_2$ ($x=0, 0.1, 0.2, 0.3$) 复合物正极材料。XRD 测试表明, 富锂锰基复合材料具有典型的 $R\bar{3}m$ 和 $C2/m$ 层状复合结构。SEM 观察表明, 颗粒粒度在 0.4~1.1 之间, 并且粒度随锂含量的增加而增大。 $\text{Li}_{1.2}(\text{Mn}_{0.6}\text{Ni}_{0.2}\text{Co}_{0.2})_{0.8}\text{O}_2$ 具有较好的首次放电容量, 在电流密度为 20 mA/g, 电压为 2.0~4.8 V 下, 其首次放电容量为 275.7 mA·h/g。然而 $\text{Li}_{1.1}(\text{Mn}_{0.6}\text{Ni}_{0.2}\text{Co}_{0.2})_{0.9}\text{O}_2$ 表现出较好的循环性能, 在 0.2C、50 次循环后, 容量保持率为 93.8%, 在反应动力学中具有较好的锂离子脱嵌能力。

关键词: 正极材料; $\text{Li}_{1+x}(\text{Mn}_{0.6}\text{Ni}_{0.2}\text{Co}_{0.2})_{1-x}\text{O}_2$; 电化学性能; 锂离子电池

(Edited by Xiang-qun LI)